Microbiome shifts during *Fusarium oxysporum* and *F. solani* (syn. *Neocosmospora solani*)—induced *Ligusticum chuanxiong* root rot: endophtic bacterial protective responses and fungal pathogenic tendencies

Weiping Gao[1,2], Hai Wang[1,3], Hongmei Jia[1,2], Jianyun Zhang[1,2], Zhuyun Yan[1,2], Dongmei He[1,2] and Chuan Zheng[1]

[1] State Key Laboratory of Characteristic Chinese Medicine Resources in Southwest China, Chengdu University of Traditional Chinese Medicine, Chengdu, Sichuan, China
[2] School of Pharmacy, Chengdu University of Traditional Chinese Medicine, Chengdu, Sichuan, China
[3] School of Medical Technology, Chengdu University of Traditional Chinese Medicine, Chengdu, Sichuan, China

ABSTRACT

Root rot disease is a globally significant threat to the health of diverse economically important crops. Understanding shifts in the plant microbiome during disease progression can aid in identifying beneficial microbes with disease-resistant potential and developing ecofriendly biocontrol strategies. However, microbiome changes during root rot progression in the medicinal plant *Ligusticum chuanxiong* remain poorly understood. This study aimed to investigate the response of host-associated microbiomes to pathogen stress (*Fusarium oxysporum* and *F. solani* syn. *Neocosmospora solani*) during *L. chuanxiong* root rot. The diversity, composition, function, and network interactions of bacterial and fungal communities were examined using high-throughput sequencing and network analysis in healthy rhizomes, healthy layers of diseased rhizomes, rotten layers of diseased rhizomes, and rhizosphere and non-rhizosphere soils. The bacterial diversity decreased as root rot progressed in end ophytic (from 0.72 to 0.38) and rhizosphere soils (from 0.80 to 0.68), whereas the fungal diversity showed no significant changes. The diseased samples were enriched with root rot pathogens and other potential pathogens, such as the soil bacterium *Pectobacterium* and the soil fungus *Gibberella*, whereas beneficial taxa, including endophytic *Bacillus* and *Trichoderma*, and soil-dwelling *Candidatus_Solibacter* and *Beauveria*, were significantly reduced. Notably, in the healthy layers of diseased rhizomes, which represent a "transitional phase", fungal communities resembled those in rotten tissues with increased pathogenic taxa (*e.g.*, *Ceratocystis* and *Plectosphaerella*), whereas bacterial communities were more similar to healthy rhizomes and enriched in beneficial genera (*e.g.*, *Microbacterium* and *Variovorax*). Functional prediction indicated suppressed bacterial activity and enhanced fungal saprotrophy in rotten rhizomes. The cross-kingdom network complexity decreased in both endophytic and soil microbial communities during root rot, while positive correlations within endophytic networks increased. Overall, as root rot progresses, the stability and competitive interactions within endophytic and soil microbiomes of *L. chuanxiong* weaken. Early in infection, endophytic bacterial and fungal communities

Submitted 13 June 2025
Accepted 18 October 2025
Published 25 November 2025

Corresponding authors
Dongmei He, hedongmei@cdutcm.edu.cn
Chuan Zheng, zhengchuan@cdutcm.edu.cn

Academic editor
Rodrigo Nunes-da-Fonseca

Additional Information and Declarations can be found on page 20

DOI **10.7717/peerj.20369**

How to cite this article Gao W, Wang H, Jia H, Zhang J, Yan Z, He D, Zheng C. 2025. Microbiome shifts during *Fusarium oxysporum* and *F. solani* (syn. *Neocosmospora solani*)—induced *Ligusticum chuanxiong* root rot: endophtic bacterial protective responses and fungal pathogenic tendencies. *PeerJ* **13**:e20369 http://doi.org/10.7717/peerj.20369

exhibit divergent responses: bacteria likely contribute to disease resistance, whereas fungi may promote pathogenesis. This findings suggest that a more beneficial role for endophytic bacteria in controlling *L. chuanxiong* root rot. Restoring microbial community complexity may offer a viable biocontrol strategy. Our findings provide a theoretical foundation for future identification of specific beneficial microbes and the development of safe biocontrol approaches.

Subjects Agricultural Science, Biodiversity, Ecology, Microbiology, Plant Science
Keywords *Ligusticum chuanxiong* Hort., Plant microbiome, Microbiome shifts, High-throughput sequencing, Root rot

INTRODUCTION

Root rot is a soil-borne disease that causes necrosis and decay of underground plant parts, posing a serious threat to the cultivation of many economically important crops worldwide. In soybeans, root rot can reduce yields by 25% to 75%, severely impacting global food security (*Qian et al., 2015*; *Lu et al., 2020*). With the growing demand for medicinal plants in both traditional and modern pharmaceutical industries, the scale of medicinal plant cultivation has expanded substantially. However, medicinal plants are primarily root and rhizome herbs and require longer growth cycles, making them particularly vulnerable to root rot. This disease not only disrupts normal plant growth but also jeopardizes the accumulation of medicinal compounds, such as ginsenosides in *Panax ginseng* (Araliaceae) and triterpenoid saponins with flavonoids in *Astragalus membranaceus* (Fabaceae) (*Han et al., 2025*). Although chemical pesticides remain a primary control method, their use often leads to adverse effects such as pesticide resistance and residue accumulation. In contrast, biological control offers an environmentally friendly and sustainable alternative and has been widely explored for managing root rot in soybean, cotton, aconitum, and other crops (*Sun et al., 2023*; *Wang et al., 2024a*; *Babu et al., 2015*).

The plant microbiome plays a vital role in plant health by promoting growth, increasing productivity, and defending against pathogens (*Hu et al., 2024*; *Zhou et al., 0000*). Healthy plant microbiomes contain diverse "disease-preventing members" that balance the ecosystem by suppressing pathogens and preventing infections (*Lv et al., 2023*). However, reduced microbial diversity and weakened connectivity can increase plant susceptibility to disease, as synergistic interactions among pathogens disrupt plant-microbe homeostasis and accelerate disease progression (*Koskella et al., 2017*; *Pitlik & Koren, 2017*). Interestingly, disease-induced shifts in the plant microbiome may also contribute to pathogen resistance. Certain beneficial microbes can prime systemic immunity in host plants, thereby enhancing disease resilience (*Yu et al., 2022*; *Li et al., 2022*). Therefore, identifying key microbial taxa involved in disease development is crucial for designing novel biocontrol agents and implementing sustainable plant protection strategies.

Ligusticum chuanxiong Hort. is a historically important medicinal and edible plant, widely used in traditional medicine for its effective headache treatment (*Committee, 2020*). Modern studies have revealed that its rhizomes are rich in bioactive compounds,

including phthalides, phenolic acids, alkaloids, and polysaccharides, which play crucial roles in managing cardiovascular and cerebrovascular diseases (*Wang et al., 2025*; *Xing et al., 2024*). In some Asian countries, its leaves are also consumed as salad greens or cooked vegetables, valued for their ability to alleviate dizziness (*Chen et al., 2018*). However, root rot poses a serious threat to *L. chuanxiong* cultivation, often causing significant yield loss or complete crop failure. The primary pathogens, *Fusarium oxysporum* and *F. solani*—the latter belonging to the *Fusarium solani* species complex, which has been proposed as a separate genus, *Neocosmospora* (*Lombard et al., 2015*)—are soil-borne fungi that infect the root system (including the rhizome) and, under warm and humid conditions, spread to the rhizomes, leading to extensive tissue decay (*Li et al., 2015*; *Li, 2016*). Disease progression is typically accompanied by shifts in the plant's microbial community, resulting in distinct microbial assemblages at early, middle, and late infection stages (*Bass et al., 2019*; *Wei et al., 2017*). Although pathogens drive disease development, plants actively recruit beneficial microbes to alleviate stress. Understanding these microbial dynamics during infection could reveal how the plant microbiome contributes to disease resistance and facilitate the identification of protective taxa. Harnessing such beneficial microbes to reshape the plant microecosystem offers a promising, sustainable strategy to promote plant health and mitigate disease.

The current understanding of microbiome dynamics during *L. chuanxiong* root rot progression remains limited. To advance knowledge in this area, we applied high-throughput sequencing to characterize bacterial and fungal microbiome shifts across three distinct disease stages: healthy, transitional (early infection), and decayed (advanced rot). By systematically analyzing diversity, structure, function, species composition, and network interactions, we revealed how the endophytic and soil microbiomes respond to pathogen stress. This study provides a theoretical basis for developing biocontrol agents against root rot and offers strategies to reduce chemical pesticide use in *L. chuanxiong* cultivation.

MATERIALS AND METHODS

Pathogen materials and inoculation procedure

The pathogens *Fusarium solani* (*Neocosmospora*) (GenBank No. KJ573076) and *F. oxysporum* (GenBank No. JN232136) were originally isolated from symptomatic *L. chuanxiong* rhizomes collected from a field plot in Shiyang Town, Sichuan Province (*Li et al., 2015*).

For inoculum preparation, both species were cultured separately on potato dextrose agar (PDA) medium at 28 °C until sporulation. Spore suspensions were adjusted to 10^5 Colony Forming Units (CFU)/mL in sterile water and mixed in equal volumes. Tissue-cultured *L. chuanxiong* seedlings were aseptically propagated through young stem nodal segment callusing (20∼40 days), shoot multiplication (25∼30 days), and root induction (25∼30 days), then transplanted into sterilized 4:1 nutrient soil:vermiculite (double-autoclaved at 121 °C for 90 min) and maintained under controlled conditions (25 °C, 14-h photoperiod, 6000 lux, 60% moisture). The experiment included eight replicates per treatment, with

5 mL of mixed spore suspension or sterile water (control) applied to each root zone (*Li et al., 2015*). Disease incidence was assessed at 14 days post-inoculation, following established criteria (*Li, 2016*), whereby rhizomes exhibiting no brown discoloration were classified as healthy, and those presenting brown lesions, tissue rotting, or hollow cavities were classified as diseased. To confirm Koch's postulates, fungi were re-isolated from symptomatic tissues and morphologically verified against the original inoculum strains.

Field Sample collection and preparation

The sampling was conducted in Shiyang town, Dujiangyan city, Sichuan Province (103°39′E, 30°50′N; Southwest China), which is the core *geo-authentic* production region of *Ligusticum chuanxiong* Hort. The sampling area experiences a typical humid subtropical monsoon climate, with an annual mean temperature of 17.1 °C, annual mean precipitation of 89 mm, a frost-free period of 269 days, and an annual sunshine duration of 1,034.6 h (*Fang et al., 2020*). Sampling was performed in mid-May 2023, coinciding with the rhizome enlargement growth stage of *L. chuanxiong*. In May, the mean daytime temperature is 26 °C, and the monthly rainfall reaches 95 mm. During this period, Sichuan experienced hot and rainy weather, leading to increased soil temperature and moisture, which coincided with the peak of *L. chuanxiong* root rot (*Li, 2016*).

Plant samples

Plant samples were collected using an equidistant sampling method, with four healthy *L. chuanxiong* plants randomly excavated from the sample field. The diseased plants were identified based on the basis of symptoms, and four symptomatic individuals were selected from the same field. The diseased plants exhibited stunted growth, with chlorotic and yellowing leaves, and the underground rhizomes showed internal browning and spongy soft rot, accompanied by a distinct sour odor. These symptoms are consistent with a wet rot pathology and align with the typical field manifestations of root rot (*Li, 2016*). Notably, residual healthy tissue, free from browning or decay, was observed within affected rhizomes. All plant samples were immediately transported to the laboratory, where the aboveground tissues and fibrous roots were removed, retaining only the rhizomes. Surface sterilization was performed by rinsing under running water, followed by immersion in 75% ethanol for 30 s and 5% sodium hypochlorite for 5 min, and then three washes with sterile water. A sterility check was included by plating the final rinse water onto Luria Bertani (LB) agar, on which no microbial growth was observed (Fig. S1). Finally, the rhizomes were longitudinally dissected under aseptic conditions in a laminar flow hood (*Sahu et al., 2022*; *He et al., 2025*; *Zhou et al., 2025*).

Three distinct tissue types were subsequently collected (Fig. 1): healthy rhizome (HR) samples were taken from healthy *L. chuanxiong* plants, with each piece including both the cortex and xylem. From diseased plants, we stratified samples into two subtypes based on pathological severity, representing different stages of infection. The diseased rhizome–healthy layer (DRH) comprises the outer, visibly non-lesioned tissue adjacent to decayed regions, reflecting early-stage infection. The diseased rhizome–rot layer (DRR) comprises the inner, fully decayed tissue, representing an advanced-stage infection that

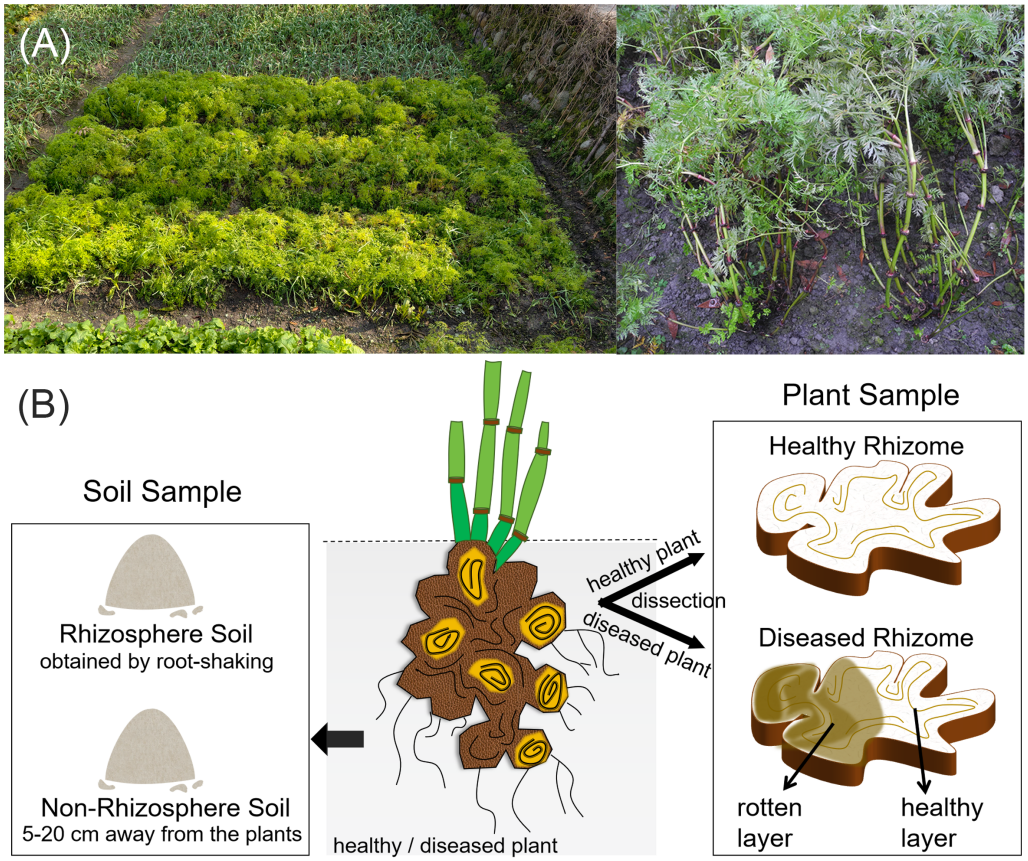

Figure 1 **Field condition and experimental sample types of *L. chuanxiong*.** (A) The field condition; (B) Representative sample types collected.

Full-size DOI: 10.7717/peerj.20369/fig-1

manifests wet rot pathology. All samples were placed in sterile tubes and stored at −20 °C for DNA extraction. There were four replicates per treatment (one replicate per individual plant).

Soil samples

Concurrently with plant sampling, rhizosphere and non-rhizosphere soils were collected (Fig. 1). Four healthy rhizosphere soil (HS) samples and four diseased rhizosphere soil (DS) samples were obtained using the root-shaking method (*Wang et al., 2024b*). After removing debris and homogenizing, the samples were placed in sterile tubes, and promptly stored at −20 °C for DNA extraction. Healthy non-rhizosphere soil (HGS) and diseased non-rhizosphere soil (DGS) samples were collected five cm to 20 cm away from the plants, and were processed following the same procedure as the rhizosphere soils. There were four replicates per treatment.

DNA extraction

The collected rhizome and soil samples were pulverized with liquid nitrogen, yielding approximately 0.1 g of each sample powder for DNA extraction using the Plant DNA

Table 1 Source and numbering of rhizome and soil samples from healthy and root rot-infected *L. chuanxiong*.

Sample type	Sample source	Sample number			
Healthy samples	Healthy rhizome	HR1	HR2	HR3	HR4
	Healthy rhizosphere soil	HS1	HS2	HS3	HS4
	Healthy non-rhizosphere soil	HGS1	HGS2	HGS3	HGS4
Diseased samples	Diseased rhizome–healthy layer	DRH1	DRH2	DRH3	DRH4
	Diseased rhizome–rot layer	DRR1	DRR2	DRR3	DRR4
	Diseased rhizosphere soil	DS1	DS2	DS3	DS4
	Diseased non-rhizosphere soil	DGS1	DGS2	DGS3	DGS4

Isolation Kit (DE-06111, Chengdu Forgene Co., Ltd.) and Soil DNA Isolation Kit (DE-055133, Chengdu Fujibiotech Co., Ltd.). The integrity, purity, and concentration of the extracted DNA were assessed by 0.8% agarose gel electrophoresis (DYY-6D, Beijing Liuyi Biotechnology Co., Ltd.) and a nucleic acid micro-spectrophotometer (DS-11+, Denovix, China). Qualified samples were subjected to high-throughput sequencing at Shanghai Majorbio Bio-Pharm Technology Co., Ltd. Detailed sample information is provided in Table 1.

PCR amplification and high-throughput sequencing

Fungi

The fungal Internal Transcribed Spacer (ITS) region was amplified using primer pair ITS1F (5′-CTTGGTCATTTAGAGGAAGTAA-3′) and ITS2R (5′-GCTGCGTTCTTCATCGATGC-3′). Polymerase chain reactions (PCRs) were performed in 20 μL volumes containing two μL of 10× Buffer, two μL of 2.5 mM dNTPs, 0.8 μL of each primer, 0.2 μL rTaq polymerase, 0.2 μL of BSA, and approximately 10 ng of template DNA, with ddH_2O added to reach the final volume. The thermal cycling conditions were as follows: initial denaturation at 95 °C for 3 min; 35 cycles of 95 °C for 30 s, 55 °C for 30 s, and 72 °C for 45 s; and followed by a final extension at 72 °C for 10 min. Each sample was amplified in triplicate, and PCR products were pooled and verified by 2% agarose gel electrophoresis. Qualified amplicons were recovered and quantified using a Qubit 2.0 fluorometer (Thermo Scientific). Libraries were prepared using the TruSeq™ DNA Sample Prep Kit (Illumina) and sequenced on the Illumina MiSeq PE300 platform.

Bacteria

The bacterial 16S rDNA V5-V7 region was amplified using a two-step PCR approach to minimize host DNA amplification. Primary amplification was performed with the primers 799F (5′-AACMGGATTAGATACCCKG-3′) and 1392R (5′-ACGGGCGGTGTGTRC-3′), followed by nested PCR with 799F and 1193R (5′-ACGTCATCCCCACCTTCC-3′). Each 20 μL PCR reaction volume contained 2.0 μL of 10× PCR buffer, 2.0 μL of 2.5 mM dNTPs, 0.8 μL each of forward and reverse primer, 0.2 μL of rTaq polymerase, 0.2 μL of BSA, 10 ng of template DNA, and ddH_2O to volume. The thermal cycling conditions were as follows: initial denaturation at 95 °C for 3 min; cycles of 95 °C for 30 s, 55 °C for 30 s, and 72 °C for 45 s; and a final extension at 72 °C for 10 min. The first PCR consisted of 27 cycles, and the

second PCR consisted of 13 cycles. The second-round PCR products were then quantified, prepared for library construction, and sequenced as described for fungal sequencing.

Statistical analysis

DNA fragments were sequenced using paired-end sequencing on the Illumina MiSeq platform. The raw sequences were processed using QIIME (v1.9.1; http://qiime.org/) for quality control and filtering. The paired-end reads from each sample were assembled using FLASH (v1.2.11; https://ccb.jhu.edu/software/FLASH/index.shtml). Operational Taxonomic Units (OTUs) were clustered at a 97% similarity threshold using UPARSE (v11; https://drive5.com/uparse/). OTUs were taxonomically classified using the Bayesian RDP classifier algorithm (v2.13; https://john-quensen.com/classifying/rdp-classifier-updated/), referencing the Silva database for bacteria (v138; https://www.arb-silva.de/) and the Unite database for fungi (v8.0; http://unite.ut.ee/index.php), respectively. Bioinformatic analyses were conducted on the Shanghai Majorbio Cloud Platform (http://www.majorbio.com) following the Mothur pipeline (v1.30.2; https://mothur.org/) with recommended parameters (*Caporaso et al., 2010*).

RESULTS

Pathogenicity of *Fusarium solani* (*Neocosmospora*) and *F. oxysporum* co-infection in *L. chuanxiong* seedlings

Pathogenicity tests revealed that co-inoculation with *F. solani* and *F. oxysporum* resulted in 100% disease incidence by 14 days post-inoculation, while control plants remained symptom-free (Fig. 2). Infected plants displayed stunted growth, leaf chlorosis, wilting, and reduced shoot formation compared to healthy controls (Figs. 2A–2D). Belowground, roots exhibited brown discoloration, tissue softening, and water-soaking lesions (Fig. 2D). Healthy rhizomes remained firm, displayed green stem scars, and released an aromatic odor upon cutting (Fig. 2E). In contrast, diseased rhizomes showed tissue softening, disintegration of vascular bundles leading to hollow cavities, and loss of characteristic aroma (Fig. 2F). Fungal isolates morphologically identical to the original inoculum strains were re-isolated from symptomatic tissues (Figs. 2G, 2H, Fig. S2), fulfilling Koch's postulates and confirming *F. solani* and *F. oxysporum* as causal agents of root rot in *L. chuanxiong*.

Analysis of the Illumina sequencing data

Microbial high-throughput sequencing was performed on three types of *L. chuanxiong* rhizome samples, representing distinct disease stages: healthy rhizome (healthy stage), healthy layer of diseased rhizome (transitional stage), and rot layer of diseased rhizome (decayed stage). Sequencing was also performed on soil samples collected from both healthy and diseased plants. After quality control, a total of 2,066,316 high-quality bacterial sequences (average length 376 bp) and 2,300,714 high-quality fungal sequences (average length 236 bp) were obtained. Clustering analysis identified 12,115 bacterial OTUs and 2,544 fungal OTUs. The saturation of rarefaction curves indicated sufficient sequencing depth (Fig. S3). Taxonomic annotation revealed that the bacterial communities spanned 38 phyla, 116 classes, 282 orders, 506 families, 1,124 genera and 2,318 species, while fungal

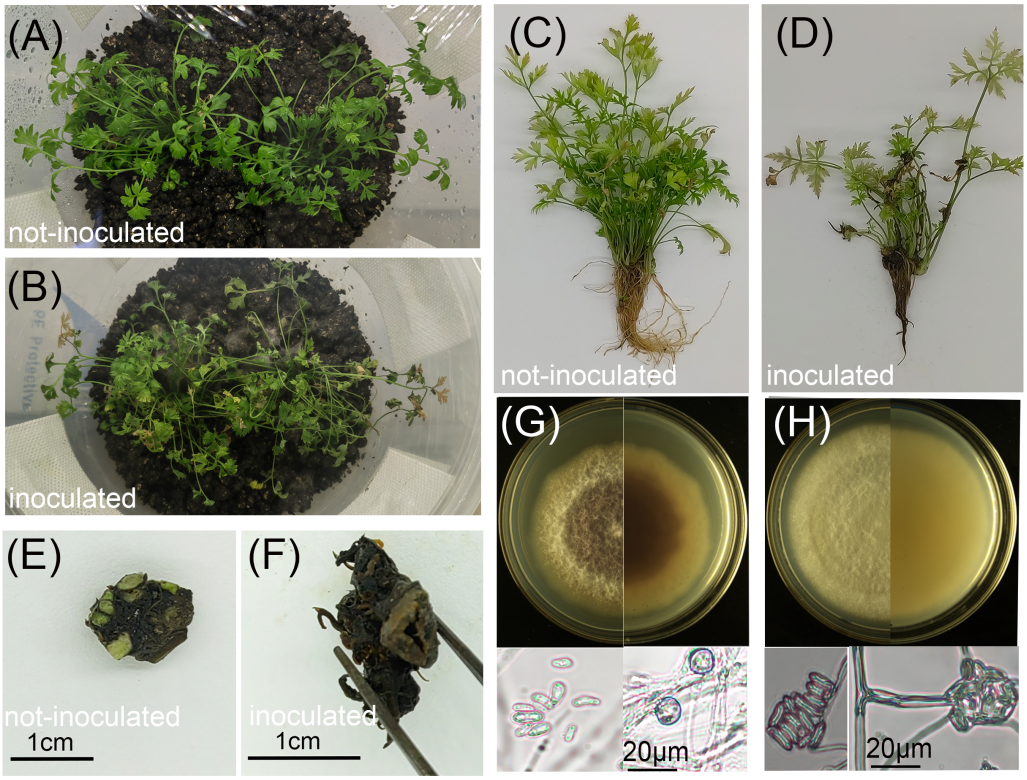

Figure 2 Effects of pathogen inoculation (*Fusarium solani* and *F. oxysporum*) on *L. chuanxiong* seedlings. (A, C) Healthy control seedlings without pathogen inoculation; (B, D) Diseased seedlings after pathogen inoculation; (E) Healthy rhizome from a control seedling; (F) Diseased rhizome from an infected seedling; (G, H) Front and reverse colony morphology and conidia of re-isolated pathogens: *F. oxysporum* (G) and *F. solani* (H).

Full-size DOI: 10.7717/peerj.20369/fig-2

communities comprised 12 phyla, 44 classes, 110 orders, 257 families, 557 genera and 904 species.

Analysis of microbial community diversity, structure, and functional characteristics during *L. chuanxiong* root rot progression

To assess changes in microbial community diversity during *L. chuanxiong* root rot progression, we analyzed alpha diversity across three disease stages (healthy, transitional, and decayed) using Kruskal–Wallis tests (Fig. 3, Table S1). For endophytic bacteria, the Ace, Shannon, and Shannon evenness indices exhibited a consistent trend: HR > DRH > DRR. Notably, HR had significantly greater diversity than DRR ($P \leq 0.01$), and DRH also had significantly higher Ace and Shannon indices than DRR ($P \leq 0.01$) (Figs. 3A–3C, blue bars). For endophytic fungi, the Shannon evenness index was significantly higher in HR compared to DRR ($P \leq 0.05$) (Fig. 3C, red bars). In the rhizosphere soil, bacterial Shannon and Shannon evenness indices were significantly greater in HS than in DS ($P \leq 0.01$) (Figs. 3E–3F, blue bars). However, no significant differences in alpha diversity were detected between healthy and diseased samples in non-rhizosphere soil microbial communities (Figs. 3D–3F).

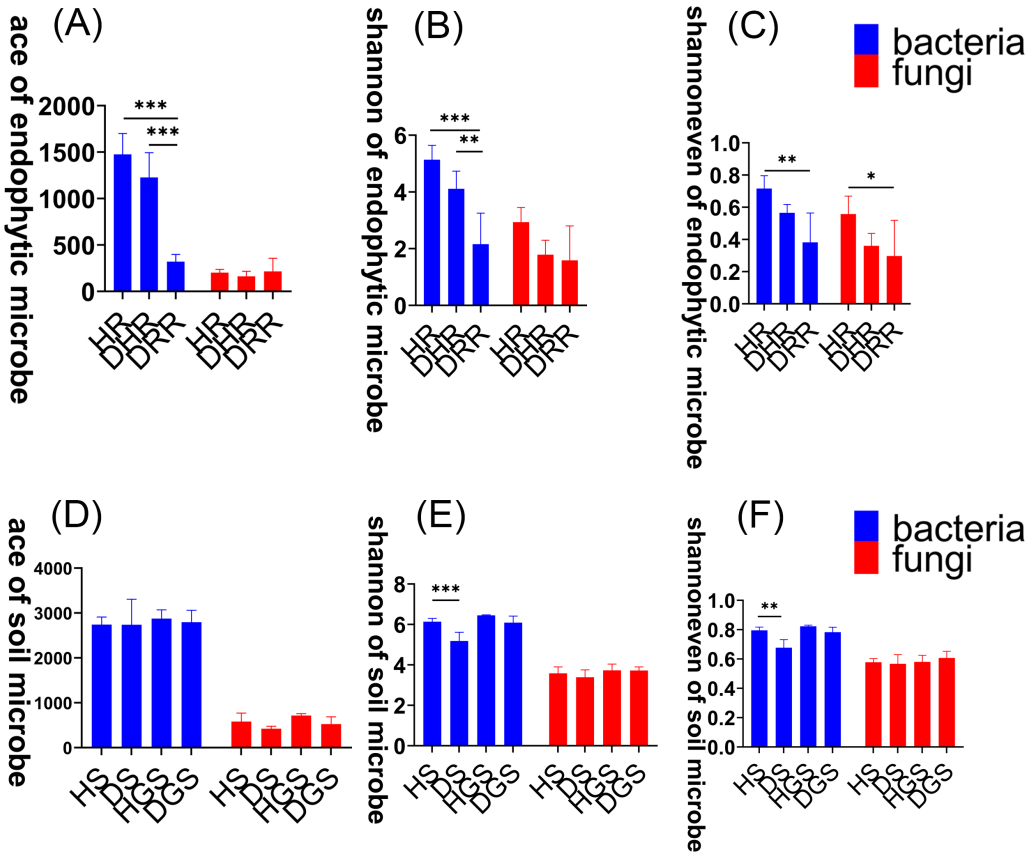

Figure 3 **Microbial alpha diversity indices in *L. chuanxiong*.** (A) ACE index of endophytic bacteria and fungi; (B) Shannon index of endophytic bacteria and fungi; (C) Shannon evenness index of endophytic bacteria and fungi; (D) ACE index of soil bacteria and fungi; (E) Shannon index of soil bacteria and fungi; (F) Shannon evenness index of soil bacteria and fungi.

Full-size DOI: 10.7717/peerj.20369/fig-3

To evaluate microbial community structural shifts during *L. chuanxiong* root rot progression, we conducted Bray-Curtis distance-based principal coordinate analysis (PCoA) (Fig. 4) and hierarchical clustering (Fig. S4). The endophytic bacterial communities clearly differed among the HR, DRH, and DRR (Fig. 4A). Similarly, soil bacterial communities formed distinct clusters in HS *vs.* DS and HGS *vs.* DGS (Figs. 4B, 4C). Endophytic fungal communities partially overlapped between DRH and DRR, but HR distinctly clustered apart from both DRH and DRR (Fig. 4D). Rhizosphere soil fungi were clearly separated between HS and DS (Fig. 4E), whereas non-rhizosphere soil fungal communities (HGS and DGS) displayed overlapping distributions (Fig. 4F). Hierarchical clustering results were consistent with the PCoA, with healthy samples clustering more tightly than diseased samples (Fig. S4). Notably, the DRH bacterial community was more similar to that of HR (Fig. S4D), whereas the DRH fungal community clustered closer to DRR (Fig. 4D).

Additionally, microbial functional changes across different pathological stages of *L. chuanxiong* were predicted using PICRUSt2 and FUNGuild analyses (Fig. 5). The bacterial

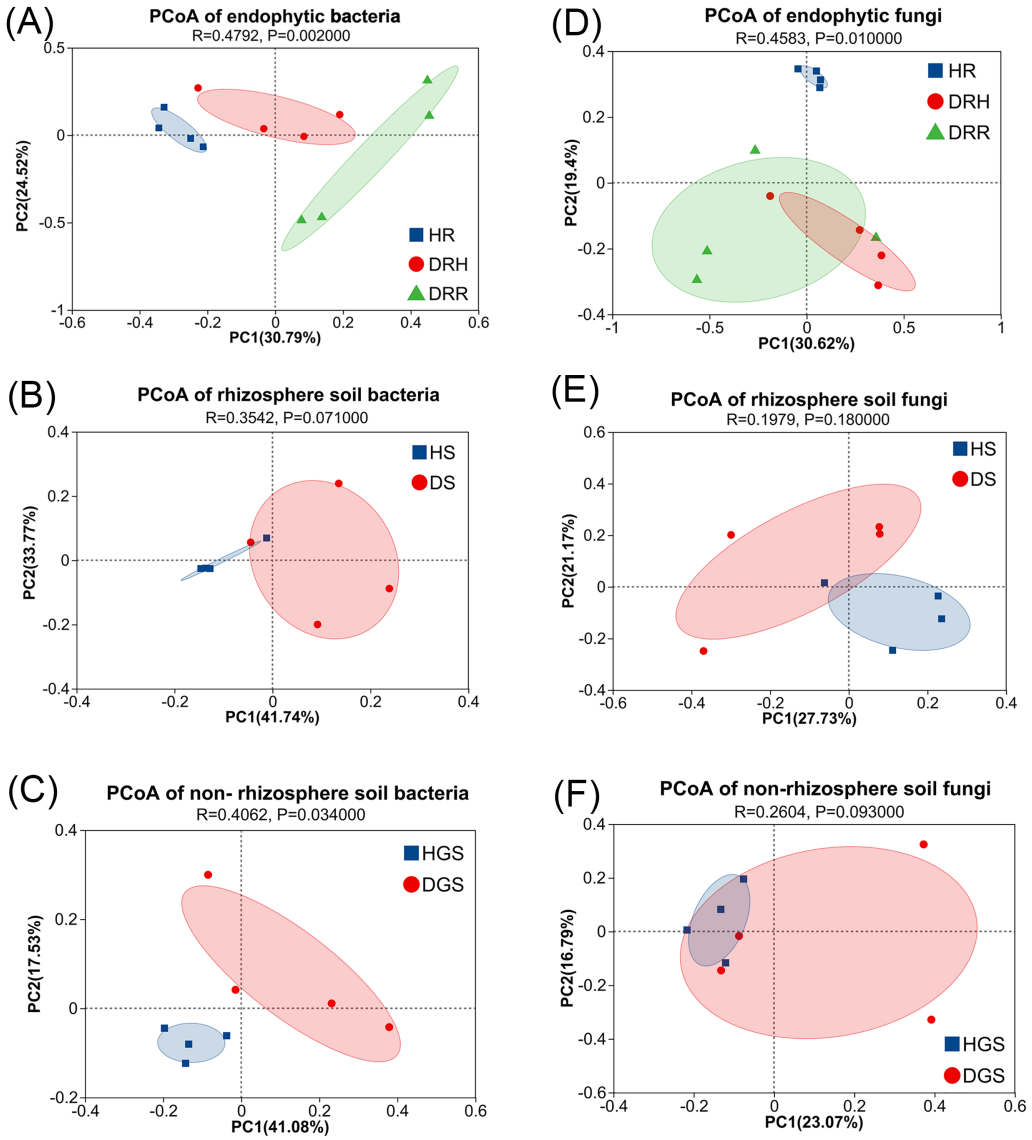

Figure 4 PCoA analysis of endophytic and soil microbial community structures during *L. chuanxiong* root rot progression. (A) Endophytic bacteria; (B) Rhizosphere soil bacteria; (C) Non-rhizosphere soil bacteria; (D) Endophytic fungi; (E) Rhizosphere soil fungi; (F) Non-rhizosphere soil fungi. The closer each sample point is, the more similar their microbial community composition.

Full-size DOI: 10.7717/peerj.20369/fig-4

PICRUSt2 analysis (Figs. 5A, 5B) revealed a decline in metabolic, environmental adaptation, and genetic information processing activities of endophytic and soil bacteria in DRR, including pathways such as biosynthesis of secondary metabolites, ABC transporters, and aminoacyl-tRNA biosynthesis. The fungal FUNGuild classification (Figs. 5C, 5D) revealed fungal trophic transitions: HR was dominated by pathotroph-saprotroph-symbiotroph fungi, DRH exhibited increased pathotroph and pathotroph-saprotroph dominance, while decayed tissues and diseased soils (DRR/DS/DGS) became predominantly saprotrophic.

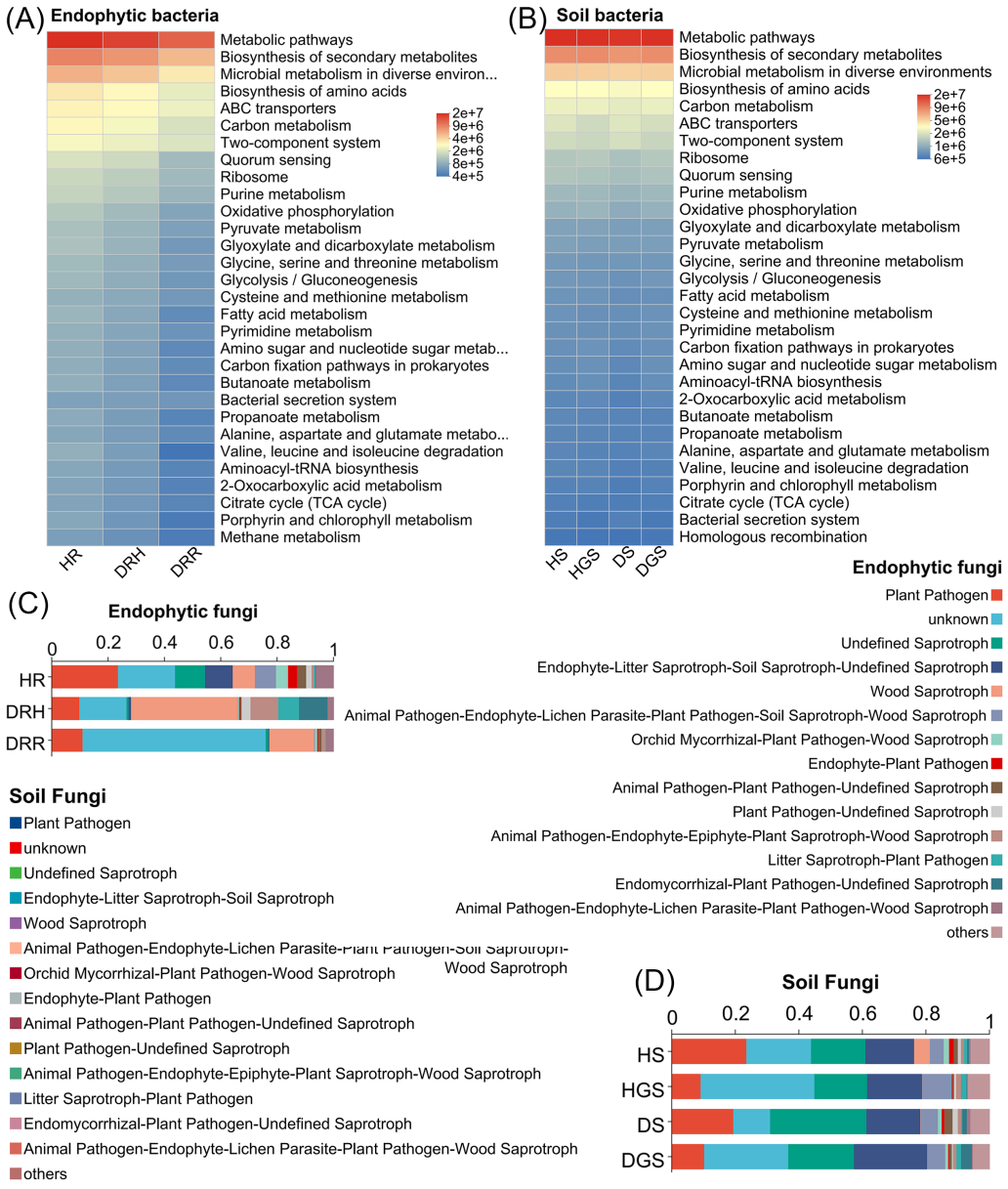

Figure 5 Functional prediction of endophytic and soil microbial communities in *L. chuanxiong* by PICRUSt 2 and FUNGuild. (A) Endophytic bacteria; (B) Soil bacteria; (C) Endophytic fungi; (D) Soil fungi.
Full-size DOI: 10.7717/peerj.20369/fig-5

In summary, the α-diversity was primarily observed in bacterial communities, with healthy rhizomes and rhizosphere soils harboring significantly richer and more diverse bacterial communities than diseased samples. Disease progression progressively reduced bacterial diversity indices, particularly in decayed tissues. The β-diversity analyses revealed distinct endophytic and rhizosphere soil microbial community structures (both bacterial and fungal) between healthy and decayed samples. Notably, at the transitional phase (DRH) from health to disease, bacterial communities remained more similar to those of healthy

rhizomes, whereas fungal communities aligned closer to decayed tissues. Furthermore, disease progression was accompanied by a reduction in bacterial functional activity and a shift of fungal communities toward saprotrophic functions.

Composition and differential analysis of microbial species during *L. chuanxiong* root rot progression

Bacterial species composition and differential analysis in L. chuanxiong

The Venn diagram revealed that endophytic bacteria represented 36.62%–44.80% differential OTUs across healthy, transitional, and decay stages (Fig. 6A), and soil bacterial communities showed 10.39%–43.34% differential OTUs between healthy and diseased samples (Fig. 6E). Further analysis focused on the relative abundance changes in the dominant bacterial taxa (relative abundance >1%) during the progression of disease in *L. chuanxiong*. At the phylum level, endophytic bacterial communities were mainly composed of seven dominant phyla (collectively accounting for >97.11% of total sequences), while soil bacterial communities comprised twelve dominant phyla (representing >98.00% of total sequences) (Figs. 6B, 6F). The relative abundance profiles of dominant bacterial genera are provided in (Figs. S5A, S5B). In healthy rhizomes (HR), the highest relative abundances were observed for Actinobacteriota, Chloroflexi, *Bacillus*, *Sphingomonas*, *Rhodococcus*, unclassified_f_Oxalobacteraceae, and norank_f_Ardenticatenaceae (all $P \leq 0.01$), as well as *Nocardioides*, *Brevundimonas*, *Streptomyces*, and *Polaromonas* (all $P \leq 0.05$). In contrast, disease transition phase (DRH) showed significantly higher abundances of Myxococcota, *Microbacterium*, *Allorhizobium-Neorhizobium-Pararhizobium-Rhizobium*, *Variovorax*, *Flavobacterium*, *Chryseobacterium*, *Devosia* (all $P \leq 0.05$), and unclassified_p_Proteobacteria ($P \leq 0.01$) (Figs. 6C, 6D). In soil samples, Chloroflexi, *Gemmatimonas*, norank_f_Xanthobacteraceae, *Acidothermus*, *Pseudolabrys*, norank_*f_norank_o_Gaiellales*, *Bryobacter*, and norank_f_norank_o_Elsterales (all $P \leq 0.01$), along with Myxococcota, *Bradyrhizobium*, *Candidatus_Solibacter*, norank_f_Methyloligellaceae, norank_f_norank_o_Acidobacteriales, *Nitrospira*, norank_f_Micropepsaceae, and *Haliangium* (all $P \leq 0.05$), were significantly enriched in healthy soils (HS, HGS). Conversely, *Pseudomonas* ($P \leq 0.01$) and *Omamonas*, *Ectobacterium*, and unclassified_f_Alcaligenaceae (all $P \leq 0.05$) presented relatively high abundances in diseased soils (DS, DGS) (Figs. 6G, 6H).

Fungal species composition and differential analysis in L. chuanxiong

The Venn diagram revealed that differential OTUs of endophytic fungi accounted for 39.40% to 47.50% of the total OTUs across different pathological stages (Fig. 7A), and differential OTUs of soil fungi ranged from 17.83% to 25.41% (Fig. 7E). Further analysis focused on changes in the relative abundance of dominant fungi (relative abundance >1%) during disease progression. Across all samples, endophytic fungi were mainly composed of four dominant phyla (accounting for more than 99.74% of total sequences), while soil fungi primarily belonged to five dominant phyla (representing more than 99.48% of total sequences) (Figs. 7B, 7F). The relative abundance profiles of dominant fungal genera are provided in the supplementary materials (Figs. S5C, S5D). In HR, the genera *Trichoderma*, *Beauveria*, *Neocosmospora*, and *Cladosporium* exhibited the highest relative abundances

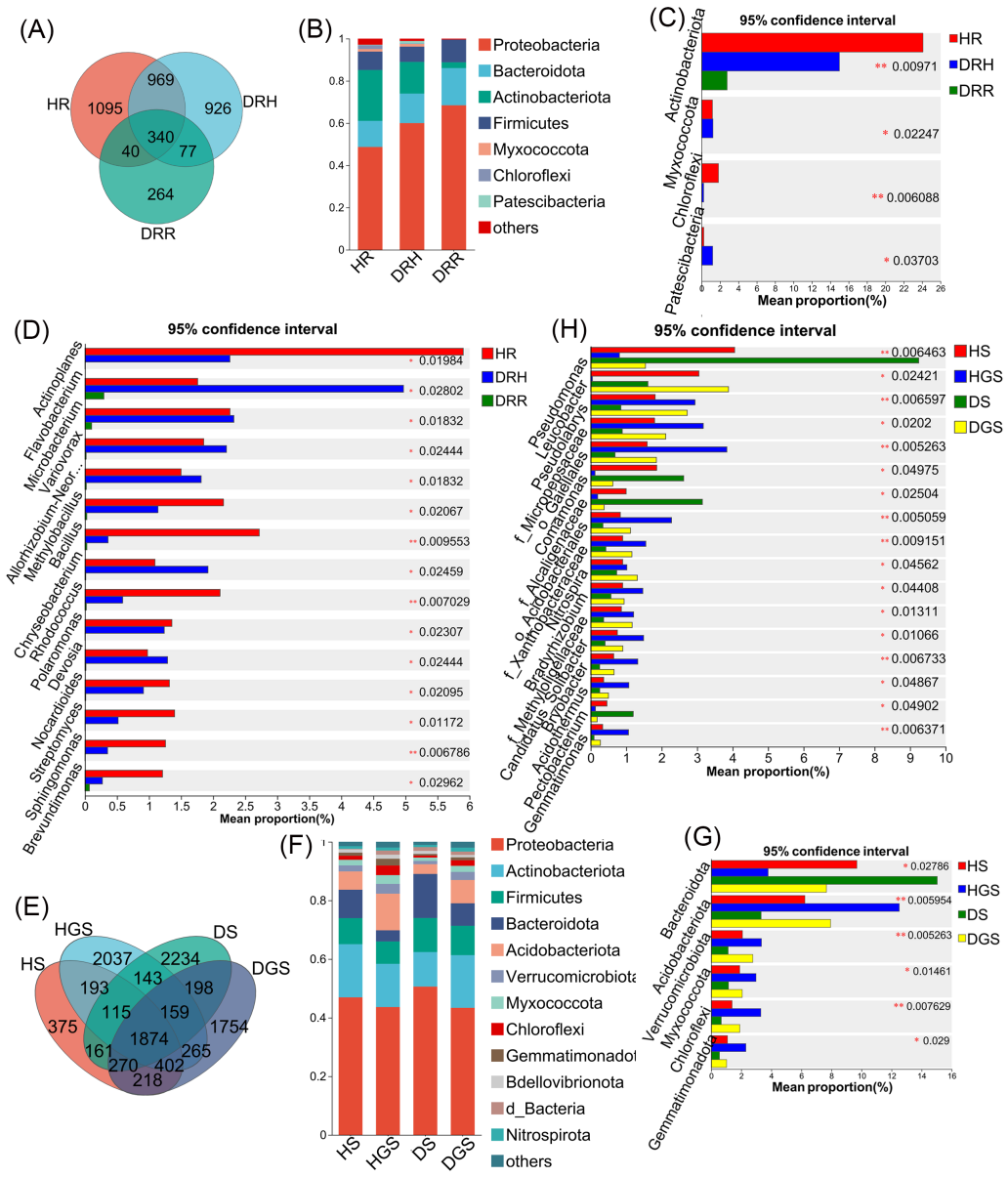

Figure 6 Composition and differential analysis of endophytic and soil bacterial communities in *L. chuanxiong* across distinct pathological stages. Venn diagrams of endophytic bacteria (A) and soil bacteria (E) at the OTU level, with numbers indicating the shared OTUs across different pathological stages; taxonomic composition of endophytic bacteria (B) and soil bacteria (F) at the phylum level; differential phyla of endophytic bacteria (C) and soil bacteria (G); differential genera of endophytic bacteria (D) and soil bacteria (H).

Full-size DOI: 10.7717/peerj.20369/fig-6

(all $P \leq 0.05$) (Fig. 7C). In DRH, *Ceratocystis* ($P \leq 0.05$) and *Plectosphaerella* showed the highest relative abundances (Fig. 7C; Fig. S5C). Among the soil samples, *Solicoccozyma* ($P \leq 0.01$), *Basidiomycota*, *Beauveria*, *Ilyonectria*, and unclassified_o_GS11 (all $P \leq 0.05$) were significantly enriched in healthy soils (HS, HGS) (Figs. 7D, 7G). Conversely, *Gibberella*,

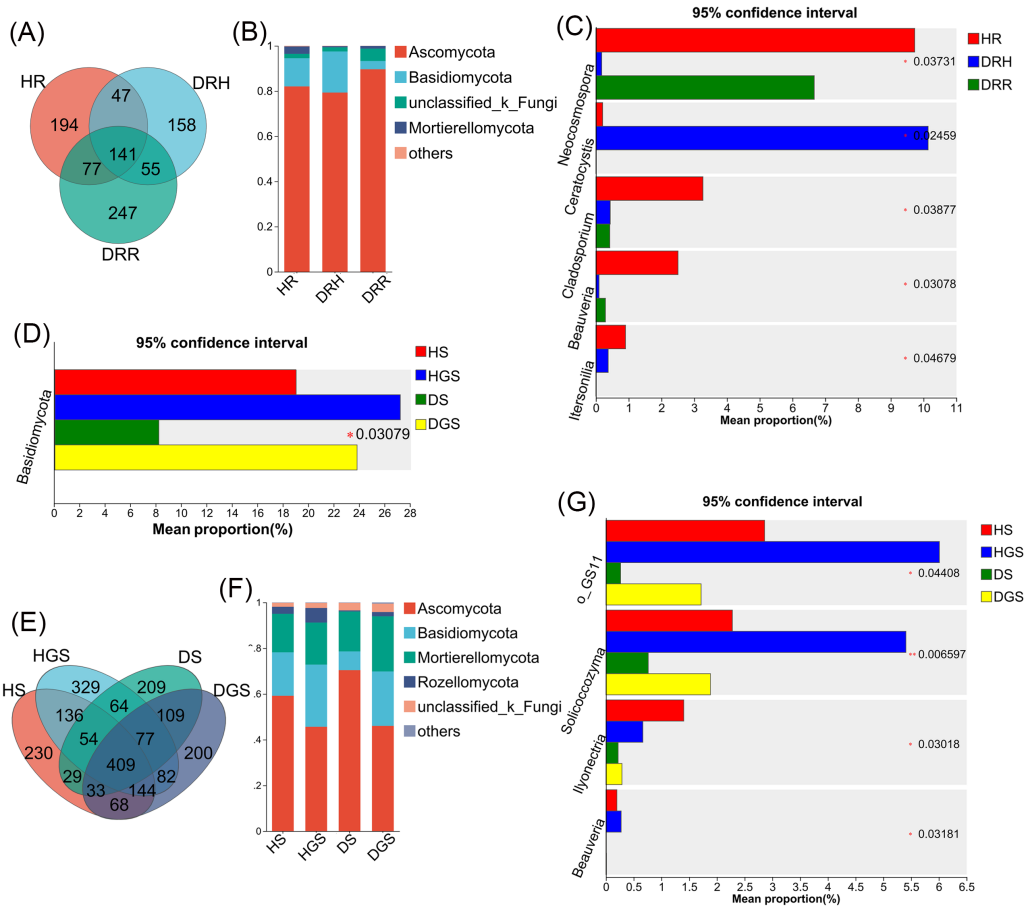

Figure 7 Composition and differential analysis of endophytic and soil fungal communities in *L. chuanxiong* across distinct pathological stages. Venn diagrams of endophytic fungi (A) and soil fungi (E) at the OTU level, with numbers indicating the shared OTUs across different pathological stages; taxonomic composition of endophytic fungi (B) and soil fungi (F) at the phylum level; differential phyla of endophytic fungi (C); differential genera of endophytic fungi (D) and soil fungi (G).

Full-size DOI: 10.7717/peerj.20369/fig-7

unclassified_f_Nectriaceae, and unclassified_f_Ceratobasidiaceae dominated in diseased soils, while their relative abundances were less than 1% in healthy soils (Fig. S5D).

Microbial co-occurrence network analysis in healthy and root rot *L. chuanxiong*

To illustrate the interaction characteristics and stability of *L. chuanxiong* microbial communities across different pathological stages, co-occurrence networks of bacteria, fungi, and cross-kingdom microbes were constructed based on Spearman correlations among dominant genera ($P < 0.05$). The number of edges (141), average degree (5.875), and network density (0.135) were higher in the endophytic bacterial co-occurrence network in healthy rhizomes (HR) than the edges (98), average degree (4.445), and network density (0.104) in rotten rhizomes (DRR) (Figs. 8A–8C). However, for the endophytic fungal network, the edges (200), average degree (4.651), and network density (0.111) were higher

in rotten rhizomes (DRR) related to the edges (71), average degree (3.302), and network density (0.079) in healthy rhizomes (HR) (Figs. 8D–8F). Notably, the proportion of positive correlations in both bacterial and fungal networks was greater in DRR (bacteria: 93.88%; fungi: 91.50%) than in HR (bacteria: 61.70%; fungi: 57.75%) (Figs. 8A–8F). Furthermore, the cross-kingdom microbial co-occurrence networks showed a decreasing trend in positive correlations, nodes, edges, average degree, and network density in the order HR >DRH >DRR (Figs. 8G–8I).

In the co-occurrence networks of soil bacteria, the average degree (HS: 4.735, HGS: 6.735) and network density (HS: 0.099, HGS: 0.140) of healthy soils were lower than the average degree (DS: 6.936, DGS: 7.064) and network density (DS: 0.151, DGS: 0.154) of diseased soils (Figs. 9A–9D). In contrast, for soil fungal networks, the average degree (HS: 3.714, HGS: 3.860) and network density (HS: 0.077, HGS: 0.092) in healthy soils were higher than the average degree (DS: 1.957, DGS: 1.978) and network density (DS: 0.043, DGS: 0.045) in diseased soils (Figs. 9E–9H). Moreover, the cross-kingdom microbial co-occurrence network revealed that the nodes (137), edges (982), average degree (14.336), and modularity (0.803) in diseased rhizosphere soil (DGS) were lower than the nodes (113), edges (726), average degree (12.850), and modularity (0.754) in healthy rhizosphere soil (HS) (Figs. 9I–9L).

In summary, endophytic bacteria and soil fungi presented increased network complexity and cohesion in healthy *L. chuanxiong* samples, whereas endophytic fungi and soil bacteria presented increased activity in decay-stage samples. Notably, the cross-kingdom interactions of endophytic and rhizosphere soil microbiomes were more stable in healthy plants, with greater microbial community activity and resilience than in diseased microbiomes. Under pathogen stress, endophytic microbiota shifted toward predominantly mutualistic relationships, while competitive and antagonistic interactions were significantly attenuated.

DISCUSSION

The plant microbiome has long been recognized as an essential part of plant ecosystem and is closely associated with plant growth and disease resistance (*Cordovez et al., 2019*). Under pathogen stress, plants can use their root exudates to recruit beneficial microbes from the environment to increase their ability to combat the stress (*Liu et al., 2020*). These exudates often include organic acids, amino acids, phenolic compounds, and other secondary metabolites, which serve as nutrients or antimicrobial agents that facilitate the colonization of beneficial rhizosphere bacteria (*Chen & Liu, 2022*). Beyond root exudates, microbe-derived metabolites are also recognized as a promising source of functional compounds in the rhizosphere. Compounds such as carbohydrates, siderophores, exopolysaccharides, and malate, released by microbes, help establish a close association between the plant and its surrounding rhizosphere microbiome, mitigating various adverse conditions (*Fan et al., 2025*). This adaptive modification of the plant-associated microbiota, often described as a plant "cry for help" response, constitutes a positive ecological strategy to mitigate stress. For instance, *Yin et al. (2021)* reported that wheat plants continuously exposed to

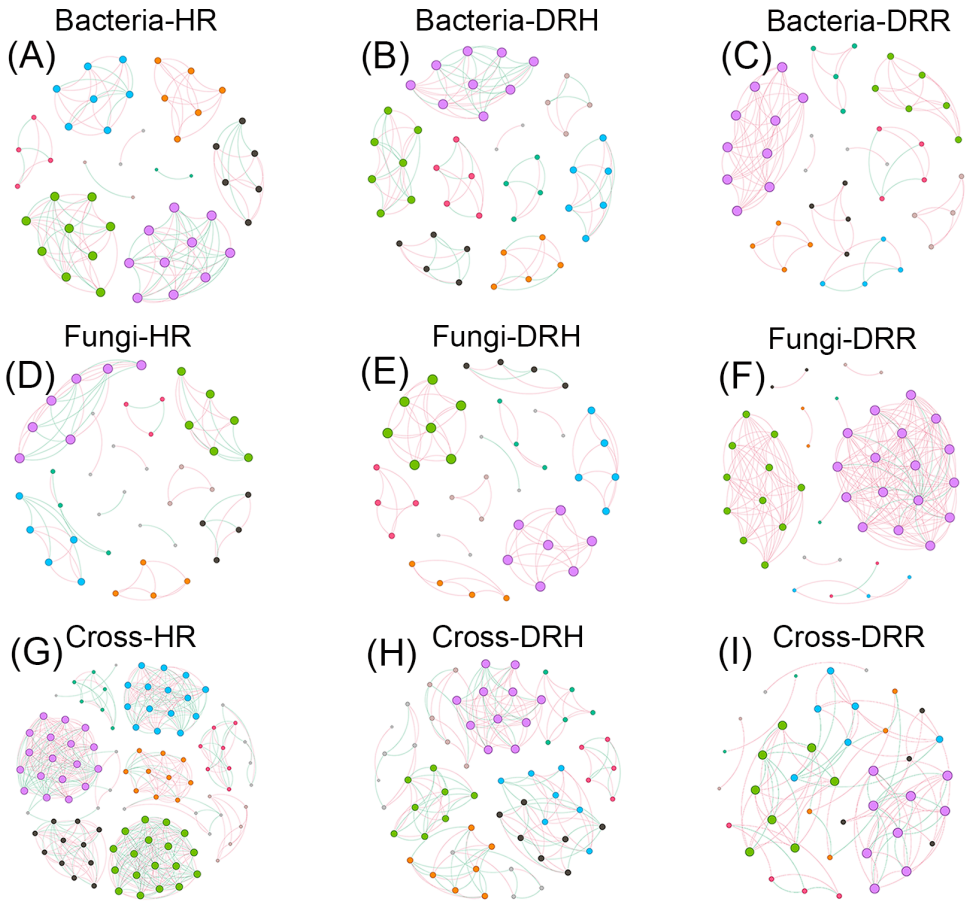

	Bacteria			Fungi			Cross-kingdom		
	HR	DRH	DRR	HR	DRH	DRR	HR	DRH	DRR
Nodes	48	47	44	43	43	43	104	65	41
Edges	114	115	98	71	79	200	576	189	100
Average Degree	5.875	4.894	4.455	3.302	3.674	4.651	11.077	5.15	4.878
Graph Density	0.125	0.106	0.104	0.079	0.087	0.111	0.108	0.091	0.022
Modularity	0.786	0.823	0.743	0.828	0.822	0.462	0.808	0.846	0.758
Positive (%)	61.70	49.57	93.88	57.75	94.94	91.50	60.94	58.73	76.00
Negative (%)	38.30	50.43	6.12	42.25	5.06	8.50	39.06	41.27	33.00

Figure 8 Co-occurrence networks of endophytic bacteria, fungi and cross-kingdom microorganisms in *L. chuanxiong* under different pathological stages. (A–C) represent endophytic bacterial networks of HR, DRH, and DRR, respectively; (D–F) represent endophytic fungal networks of HR, DRH, and DRR, respectively; (G–I) represent endophytic cross-kingdom networks of HR, DRH, and DRR, respectively. Different node colors indicate distinct modules. Red edges represent positive correlations, while blue edges indicate negative correlations. Abbreviations: HR, healthy rhizome; DRH, healthy layer of diseased rhizome; DRR, rot layer of diseased rhizome.

Full-size DOI: 10.7717/peerj.20369/fig-8

pathogenic fungi can reshape their rhizosphere microbial communities, particularly by recruiting beneficial microbes to suppress soil-borne fungal pathogens and promote plant growth. Similar plant-driven assembly of disease-suppressive microbiomes had also been

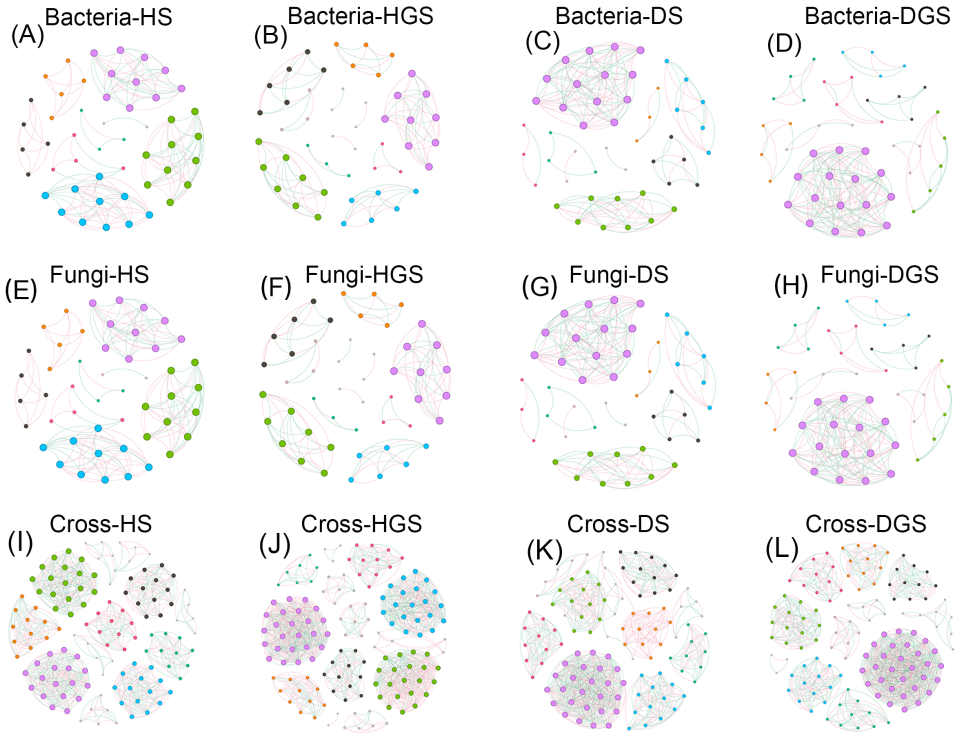

	Bacteria				Fungi				Cross-kingdom			
	HS	HGS	DS	DGS	HS	HGS	DS	DGS	HS	HGS	DS	DGS
Nodes	49	49	47	47	49	43	46	45	137	122	113	124
Edges	165	116	163	166	91	83	90	89	982	696	726	890
Average Degree	6.735	4.735	6.936	7.064	3.714	3.86	1.957	1.978	14.336	11.41	12.85	14.355
Graph Density	0.140	0.099	0.151	0.154	0.077	0.092	0.043	0.045	0.105	0.094	0.115	0.117
Modularity	0.768	0.802	0.626	0.467	0.861	0.834	0.85	0.813	0.803	0.853	0.754	0.694
Positive (%)	58.79	52.59	49.69	48.19	56.04	51.81	53.33	46.07	59.88	51.29	54.68	50.45
Negative (%)	41.21	47.41	50.31	51.81	43.96	48.19	46.67	53.93	40.12	48.71	45.32	49.55

Figure 9 Co-occurrence networks of soil bacteria, fungi and cross-kingdom microorganisms in *L. chuanxiong* under different pathological stages. (A, B) represent bacterial networks of healthy rhizosphere and non- rhizosphere soils; (C, D) bacterial networks of diseased rhizosphere and non- rhizosphere soils; (E, F) fungal networks of healthy rhizosphere and non- rhizosphere soils; (G, H) fungal networks of diseased rhizosphere and non- rhizosphere soils; (I, J) cross- kingdom networks of healthy rhizosphere and non- rhizosphere soils; (K, L) cross- kingdom networks of diseased rhizosphere and non- rhizosphere soils. Different node colors represent distinct modules. Red edges indicate positive correlations, while blue edges represent negative correlations. Abbreviations: HS, healthy rhizosphere soil; HGS, healthy non- rhizosphere soil; DS, diseased rhizosphere soil; DGS, diseased non- rhizosphere soil.

Full-size DOI: 10.7717/peerj.20369/fig-9

observed in tomato crops, underscoring the broader relevance of this phenomenon across different plant species (*Peng et al., 2025*). Collectively, these dynamic shifts in microbial community composition hold potential for addressing agronomic challenges related to plant diseases.

This study investigated shifts in the microbial communities among healthy *L. chuanxiong* plants, the healthy layer of diseased plants, and the decayed layer. At the phylum level, we observed significant depletion of Chloroflexi and Myxococcota in diseased rhizomes and surrounding soil. These phyla include diverse predatory bacterial groups capable of

consuming various bacteria and fungi, while possessing antimicrobial secondary metabolite biosynthesis potential, making them agriculturally valuable for biological control (*Du et al., 2023*; *Xian, Zhang & Li, 2020*). At the genus level, as disease severity increased, the relative abundances of potentially beneficial microbes, including *Bacillus* (0.03%), *Trichoderma* (0.89%), and *Beauveria* (0.29%), declined markedly, all falling below 1%. Notably, *Bacillus* and *Trichoderma* species are widely utilized as biocontrol agents against plant fungal pathogens (*Zanon et al., 2024*; *Harman, 2008*), while the entomopathogen *Beauveria* promotes plant growth and suppresses *Fusarium*-induced crown rot in wheat (*Jaber, 2018*). Conversely, the abundance of pathogenic and potentially pathogenic genera, including *Gibberella* and *Pectobacterium*, significantly increased. *Gibberella* represents the sexual reproductive stage of certain *Fusarium* species, that were originally identified in rice bakanae disease (*Crous et al., 2022*). Many members of these genera are recognized plant pathogens (*Zhang et al., 2023*), including *F. oxysporum*, *F. solani*, and *F. asiaticum*, which have been implicated in *L. chuanxiong* root rot (*Li et al., 2015*; *Zhu et al., 2022*). *Pectobacterium*, a broad-host-range bacterial pathogen, primarily causes soft rot diseases through critical virulence factors like cell wall-degrading enzymes (*Li et al., 2019*). Importantly, our findings corroborate previous studies identifying *Bacillus* and *Trichoderma* as key differential taxa between healthy and diseased *L. chuanxiong* rhizosphere microbiomes (*Sun et al., 2024*), highlighting their promising potential for developing biocontrol strategies against root rot.

Notably, the "transition phase" (the healthy layer of diseased rhizomes) exhibited dual-phase microbial community shifts during root rot progression. This ecotone harbored an increased abundance of potentially pathogenic fungi, including *Ceratocystis*, the primary causal agent of sweet potato black rot (*Wang, Tian & Liu, 2023*; *Wang, TIan & Liu, 2023*), and *Plectosphaerella*, which is associated with stunting disease in tomato and pepper crops (*Raimondo & Carlucci, 2017*). In contrast to the fungal community shifts, the bacterial community structure at this transition phase more closely resembled that of healthy rhizomes, showing selective enrichment of potentially beneficial taxa: *Microbacterium*, *Variovorax*, *Allorhizobium-Neorhizobium-Pararhizobium-Rhizobium*, *Flavobacterium*, and *Chryseobacterium*. In addition, *Microbacterium* demonstrates remarkable environmental adaptability across wide temperature, salinity, and pH ranges, aiding plant stress tolerance (*Zhao et al., 2024*); *Variovorax* modulates phytohormone homeostasis to maintain root architecture development (*Finkel et al., 2020*); while *Rhizobium spp.* exhibit high nitrogenase activity and serve as effective biofertilizers (*Shameem et al., 2022*). Additionally, *Flavobacterium* and *Chryseobacterium* have demonstrated antagonistic activity against sugar beet wilt and rice blast diseases, respectively (*Carrión et al., 2019*; *Kumar et al., 2021*). Overall, the enrichment of beneficial bacteria in the healthy layer of diseased *L. chuanxiong* rhizomes suggests that, during the early pathogen invasion, the plant may actively restructure its microbiome to recruit and accumulate advantageous bacteria, thereby enhancing resistance and delaying disease progression. These findings are consistent with those of *Carrión et al. (2019)* who showed that pathogen-induced endophytic bacteria suppress fungal diseases through activation of specific biosynthetic gene clusters, as confirmed by transcriptomic analyses. Therefore, future studies on synthetic microbial consortia for combating *L. chuanxiong* root rot should incorporate these beneficial bacterial

taxa to validate their role in enhancing host resistance. Such efforts will not only advance our understanding of plant-microbe interactions but also provide a theoretical foundation for developing novel biocontrol strategies leveraging beneficial bacteria.

Microbial community structure and function are dynamically regulated by interaction networks, where increased network complexity typically correlates with enhanced metabolic activity and ecosystem resilience (*Gao et al., 2021*; *Wagg et al., 2019*). In this study, root rot infection in *L. chuanxiong* substantially destabilized rhizosphere microbial networks across kingdoms, coinciding with reduced bacterial functional activity and fungal community transition toward saprotrophic dominance. These findings highlight microbiome stability as a critical determinant of plant health. Concurrently, microbial networks in diseased rhizomes showed increased positive correlations, reflecting pathogen enrichment alongside opportunistic colonizers of necrotic tissue. While this pattern implies strengthened cooperative interactions among surviving microbiota (*Herren & McMahon, 2017*), established ecological theory posits that competitive networks typically promote community stability and stress resistance (*Coyte, Schluter & Foster, 2015*). The observed reduction in competitive interactions within the diseased L. chuanxiong microbiome likely explains both the network instability and functional dysbiosis, potentially creating favorable conditions for pathogen expansion. It should be noted that functional predictions derived from genus-level taxonomy (*via* PICRUSt2/FUNGuild) represent hypothetical capacities rather than demonstrated activities. Experimental validation remains essential to confirm these metabolic inferences. Nevertheless, our findings reinforce that maintaining plant health relies on the assembly of a diverse and intricate microbial community, rather than the simple introduction of one or a few microbial taxa (*Wang et al., 2024b*). In summary, this study elucidates the shifts in endophytic and soil microbial communities during the onset and progression of *L. chuanxiong* root rot, highlighting the disease-suppressive potential of endophytic bacterial assemblages in the early stages of infection. Future research should focus on designing targeted synthetic consortia of beneficial bacteria based on pathogen-induced microbial shifts, followed by validation of their disease-suppressive effects through pot experiments and long-term field trials.

CONCLUSION

This study elucidates the response characteristics of microbial communities during the progression of *Ligusticum chuanxiong* root rot, providing a theoretical foundation for developing microecological control strategies against this disease. Under pathological conditions, the imbalance of endophytic and soil microecosystems in *L. chuanxiong* is accompanied by decreased bacterial diversity and functional activity, along with weakened stability of cross-kingdom bacterial-fungal interaction networks and reduced competitive constraints. Comparative analysis revealed significant depletion of potentially beneficial microbial taxa in diseased plants (*e.g.*, endophytic *Bacillus* and *Trichoderma*, soil-dwelling *Candidatus_Solibacter* and *Beauveria*) alongside enrichment of potential pathogens (*e.g.*, soil-borne *Pectobacterium* and *Gibberella*). Notably, rhizome-rotted *L. chuanxiong* did not completely lose beneficial microbiota. During the health-to-disease transition phase, endophytic communities exhibit dualistic dynamics: bacterial

communities demonstrate disease-suppressive potential with increased beneficial taxa (*e.g.*, *Microbacterium* and *Variovorax*), while fungal communities shift toward pathogenicity with enriched deleterious species (*e.g.*, *Ceratocystis* and *Plectosphaerella*). These findings suggest that endophytic bacteria may play more protective roles than fungi in terms of root rot resistance. Crucially, the holistic assembly of microbial communities rather than individual species mainten *L. chuanxiong* health.

ADDITIONAL INFORMATION AND DECLARATIONS

Funding

This work was supported by grants from the Natural Science Foundation of Sichuan Provence, China (No. 2025ZNSFSC0612, 2023NSFSC1994); and the National Natural Science Foundation of China (Nos. 81673553, 81001610). The funders had no role in study design, data collection and analysis, decision to publish, or preparation of the manuscript.

Grant Disclosures

The following grant information was disclosed by the authors:
Natural Science Foundation of Sichuan Provence, China: 2025ZNSFSC0612, 2023NSFSC1994.
National Natural Science Foundation of China: 81673553, 81001610.

Competing Interests

The authors declare there are no competing interests.

Author Contributions

- Weiping Gao conceived and designed the experiments, performed the experiments, analyzed the data, prepared figures and/or tables, authored or reviewed drafts of the article, and approved the final draft.
- Hai Wang analyzed the data, authored or reviewed drafts of the article, supervised the data analysis, and approved the final draft.
- Hongmei Jia analyzed the data, authored or reviewed drafts of the article, supervised the data analysis, and approved the final draft.
- Jianyun Zhang analyzed the data, authored or reviewed drafts of the article, and approved the final draft.
- Zhuyun Yan analyzed the data, authored or reviewed drafts of the article, supervised the data analysis, and approved the final draft.
- Dongmei He conceived and designed the experiments, analyzed the data, authored or reviewed drafts of the article, provided project funding support, and approved the final draft.
- Chuan Zheng analyzed the data, authored or reviewed drafts of the article, provided project funding support, and approved the final draft.

DNA Deposition

The following information was supplied regarding the deposition of DNA sequences:

The raw sequence data are available at NCBI BioProject: PRJNA1258702, PRJNA1258699, KJ573076, JN232136.

Data Availability

The following information was supplied regarding data availability:

The data is available in the Supplemental Files.

The raw sequence data are available at NCBI BioProject: PRJNA1258702, PRJNA1258699, KJ573076, JN232136.

Supplemental Information

Supplemental information for this article can be found online at http://dx.doi.org/10.7717/peerj.20369#supplemental-information.

REFERENCES

Babu S, Bidyarani N, Chopra P, Monga D, Kumar R, Prasanna R, Kranthi S, Saxena AK. 2015. Evaluating microbe-plant interactions and varietal differences for enhancing biocontrol efficacy in root rot disease challenged cotton crop. *European Journal of Plant Pathology* **142**:345–362 DOI 10.1007/s10658-015-0619-6.

Bass D, Stentiford GD, Wang H-C, Koskella B, Tyler CR. 2019. The pathobiome in animal and plant diseases. *Trends in Ecology & Evolution* **34(11)**:996–1008 DOI 10.1016/j.tree.2019.07.012.

Caporaso JG, Kuczynski J, Stombaugh J, Bittinger K, Bushman FD, Costello EK, Fierer N, Peña AG, Goodrich JK, Gordon JI, Huttley GA, Kelley ST, Knights D, Koenig JE, Ley RE, Lozupone CA, McDonald D, Muegge BD, Pirrung M, Reeder J, Sevinsky JR, Turnbaugh PJ, Walters WA, Widmann J, Yatsunenko T, Zaneveld J, Knight R. 2010. QIIME allows analysis of high-throughput community sequencing data. *Nature Methods* **7(5)**:335–336 DOI 10.1038/nmeth.f.303.

Carrión VJ, Perez-Jaramillo J, Cordovez V, Tracanna V, De Hollander M, Ruiz-Buck D, Mendes LW, Van Ijcken WFJ, Gomez-Exposito R, Elsayed SS, Mohanraju P, Arifah A, Van der Oost J, Paulson JN, Mendes R, Van Wezel GP, Medema MH, Raaijmakers JM. 2019. Pathogen-induced activation of disease-suppressive functions in the endophytic root microbiome. *Science* **366(6465)**:606–612 DOI 10.1126/science.aaw9285.

Chen L, Liu YP. 2022. The function of root exudates in the root colonization by beneficial soil rhizobacteria. *Biology* **13(2)**:95 DOI 10.3390/biology13020095.

Chen ZJ, Zhang C, Gao F, Fu Q, Fu CM, He Y, Zhang JM. 2018. A systematic review on the rhizome of Ligusticum chuanxiong Hort, (Chuanxiong). *Food and Chemical Toxicology* **119**:309–325 DOI 10.1016/j.fct.2018.02.050.

Committee TP. 2020. In: The Pharmacopoeia Committee, ed. *Pharmacopoeia of the People's Republic of China 2020 edition (Volume I)*. Beijing: China Medicine Science and Technology Press, 139.

Cordovez V, Dini-Andreote F, Carrión VJ, Raaijmakers JM. 2019. Ecology and evolution of plant microbiomes. *Annual Review of Microbiology* **73(1)**:69–88 DOI 10.1146/annurev-micro-090817-062524.

Coyte KZ, Schluter J, Foster KR. 2015. The ecology of the microbiome: networks, competition, and stability. *Science* **350(6261)**:663–666 DOI 10.1126/science.aad2602.

Crous PW, Lombard L, Sandoval-Denis M, Seifert KA, Schroers HJ, Chaverri P, Thines M. 2022. Fusarium: more than a node or a foot-shaped basal cell. *Studies in Mycology* **98**:100116 DOI 10.1016/j.simyco.2021.100116.

Du XR, JJ ANG, Ran Q, Li YZ. 2023. Myxobacteria resources and their systematic classification. *Microbiology China* **50(07)**:3104–3121 DOI 10.13344/j.microbiol.china.220983.

Fan XY, Ge AH, Qi SS, Guan YF, Wang R, Yu N, Wang E. 2025. Root exudates and microbial metabolites: signals and nutrients in plant-microbe interactions. *Science China Life Sciences* **68(8)**:2290–2302 DOI 10.1007/s11427-024-2876-0.

Fang QM, Peng WF, Wu P, Zhao JN, Wang HS, Hua Y, Ni LY, Yang Z, Tian JL. 2020. Research progress on the production regionalization of genuine medicinal materials in Luochuan. *China Journal of Chinese Materia Medica* **45(04)**:720–731 DOI 10.19540/j.cnki.cjcmm.20200104.101.

Finkel OM, Salas-González I, Castrillo G, Conway JM, Law TF, Teixeira PJPL, Wilson ED, Fitzpatrick CR, Jones CD, Dangl JL. 2020. A single bacterial genus maintains root growth in a complex microbiome. *Nature* **19(03)**:2778 DOI 10.1038/s41586-020-2778-7.

Gao M, Xiong C, Gao C, Tsui CKM, Wang MM, Zhou X, Zhang AM, Cai L. 2021. Disease-induced changes in plant microbiome assembly and functional adaptation. *Microbiome* **9**:1–18 DOI 10.1186/s40168-021-01138-2.

Han Y, Sun T, Tang Y, Yang M, Gao W, Wang L, Sui C. 2025. Root rot in medicinal plants: a review of extensive research progress. *Frontiers in Plant Science* **15**:1504370 DOI 10.3389/fpls.2024.1504370.

Harman GE. 2008. Overview of mechanisms and uses of Trichoderma spp. *Phytopathology* **113**:190–195 DOI 10.1094/phyto-96-0190.

He DM, Gao WP, Zhang ZL, Xing JN, Han GQ, Wang H, Yan ZY. 2025. Microecological recombination of Angelica sinensis driven by th e transplanting of alpine seedling-cellar planting-dam cultivation. *PeerJ* **13**:e19208 DOI 10.7717/peerj.19208.

Herren CM, McMahon KD. 2017. Cohesion: a method for quantifying the connectivity of microbial communities. *The ISME Journal* **11(11)**:2426–2438 DOI 10.1038/ismej.2017.91.

Hu D, Zhou XH, Ma GY, Pan JH, Ma HA, Chai YF, Li YS, Yue M. 2024. Increased soil bacteria-fungus interactions promote soil nutrient availability, plant growth, and co-existence. *Science of the Total Environment* **955**:176919 DOI 10.1016/j.scitotenv.2024.176919.

Jaber LR. 2018. Seed inoculation with endophytic fungal entomopathogens promotes plant growth and reduces crown and root rot (CRR) caused by Fusarium culmorum in wheat. *Planta* **45(17)**:2991 DOI 10.1007/s00425-018-2991-x.

Koskella B, Meaden S, Crowther WJ, Leimu R, Metcalf CJE. 2017. A signature of tree health? Shifts in the microbiome and the ecological drivers of horse chestnut bleeding canker disease. *New Phytologist* **215(2)**:737–746 DOI 10.1111/nph.14560.

Kumar M, Charishma K, Sahu KP, Sheoran N, Patel A, Kundu A, Kumar A. 2021. Rice leaf associated Chryseobacterium species: an untapped antagonistic flavobacterium displays volatile mediated suppression of rice blast disease. *Biological Control* **161**:104703 DOI 10.1016/j.biocontrol.2021.104703.

Li JS. 2016. Investigation on root rot of Chuanxiong and identification of pathogenic bacteria. Master thesis, Chengdu University of Traditional Chinese Medicine.

Li JS, Yan ZY, Lan Y, Shen XF, Wang H, He DM. 2015. Pathogen identification of root rot of Ligusticum chuanxiong in main producing areas of Sichuan. *Journal of Chinese Medicinal Materials* **38(03)**:443–446 DOI 10.13863/j.issn1001-4454.2015.03.004.

Li L, Yuan L, Shi Y, Xie X, Chai A, Wang Q, Li B. 2019. Comparative genomic analysis of Pectobacterium carotovorum subsp. brasiliense SX309 provides novel insights into its genetic and phenotypic features. *BMC Genomics* **89(11)**:5831 DOI 10.1186/s12864-019-5831-x.

Li PD, Zhu ZR, Zhang YZ, Xu JP, Wang HK, Wang ZY, Li HY. 2022. The phyllosphere microbiome shifts toward combating melanose pathogen. *Microbiome* **10(1)**:56 DOI 10.1186/s40168-022-01234-x.

Liu H, Brettell LE, Qiu Z, Singh BK. 2020. Microbiome-mediated stress resistance in plants. *Trends in Plant Science* **25(8)**:733–743 DOI 10.1016/j.tplants.2020.03.014.

Lombard L, van der Merwe NA, Groenewald JZ, Crous PW. 2015. Generic concepts in Nectriaceae. *Studies in Mycology* **80**:189–245 DOI 10.1016/j.simyco.2014.12.002.

Lu CC, Guo N, Yang C, Sun HB, Cai BY. 2020. Transcriptome and metabolite profiling reveals the effects of Funneliformis mosseae on the roots of continuously cropped soybeans. *BMC Plant Biology* **20(1)**:479 DOI 10.1186/s12870-020-02647-2.

Lv T, Zhan C, Pan Q, Xu H, Fang H, Wang M, Matsumoto H. 2023. Plant pathogenesis: toward multidimensional understanding of the microbiome. *IMeta* **2(3)**:e129 DOI 10.1002/imt2.129.

Peng J, Hou J, Liu H, Mavrodi DV, Mavrodi OV, Sun F, Shen M, Wang X, Dang K, Yan M, Liang H, Dong Y, Li J. 2025. Changes in the soil and rhizosphere microbiomes associated with bacterial wilt decline in the tomato monoculture field. *Geoderma* **457**:117273 DOI 10.1016/j.geoderma.2025.117273.

Pitlik SD, Koren O. 2017. How holobionts get sick-toward a unifying scheme of disease. *Microbiome* **5(1)**:64 DOI 10.1186/s40168-017-0281-7.

Qian L, Yu WJ, Cui JQ, Jie WG, Cai BY. 2015. Funneliformis mosseaeaffects the root rot pathogen: *Fusarium oxysporumin* soybeans. *Acta Agriculturae ScandInavica Section B, Soil and Plant Science* **65**:4 DOI 10.1080/09064710.2015.1009938.

Raimondo ML, Carlucci A. 2017. Characterisation and pathogenicity assessment of Plectosphaerella species associated with stunting disease on tomato and pepper crops in Italy. *Plant Pathology* **67(3)**:626–641 DOI 10.1111/ppa.12766.

Sahu PK, Tilgam J, Mishra S, Hamid S, Gupta A, J K, Verma SK, Kharwar RN. 2022. Surface sterilization for isolation of endophytes: ensuring what (not) to grow. *Journal of Basic Microbiology* **62(6)**:647–668 DOI 10.1002/jobm.202100462.

Shameem MR, Sonali JMI, Kumar PS, Rangasamy G, Gayathri KV, Parthasarathy V. 2022. Rhizobium mayense sp. Nov. an efficient plant growth-promoting nitrogen-fixing bacteria isolated from rhizosphere soil. *Environmental Research* **220**:115200 DOI 10.1016/j.envres.2022.115200.

Sun XF, Liu Y, He L, Kuang ZY, Dai SD, Hua LX, Jiang QP, Wei TY, Ye PS, Zeng HL. 2024. Response of yields, soil physiochemical characteristics, and the rhizosphere microbiome to the occurrence of root rot caused by fusarium solani in Ligusticum chuanxiong hort. *Microorganisms* **42(10)**:85–88 DOI 10.3390/microorganisms12112350.

Sun L, Wang W, Zhang X, Gao ZC, Cai SS, Wang S, Li YG. 2023. Bacillus velezensis BVE7 as a promising agent for biocontrol of soybean root rot caused by *Fusarium oxysporum*. *Frontiers in Microbiology* **14**:1275986 DOI 10.3389/fmicb.2023.1275986.

Wagg C, Schlaeppi K, Banerjee S, Kuramae EE, Van der Heijden MGA. 2019. Fungal-bacterial diversity and microbiome complexity predict ecosystem functioning. *Nature Communications* **10(1)**:4841 DOI 10.1038/s41467-019-12798-y.

Wang W, Portal-Gonzalez N, Wang X, Li J, Li H, Portieles R, Borras-Hidalgo O, He WX, Santos-Bermudez R. 2024b. Metabolome-driven microbiome assembly determining the health of ginger crop (*Zingiber officinale* L. Roscoe) against rhizome rot. *Microbiome* **12(1)**:167 DOI 10.1186/s40168-024-01885-y.

Wang Q, Qiu YJ, Wang SY, Gou YM, Hou HJ, Su TW, Zou L, Huang J. 2024a. Effective control of southern blight and root rot of *Aconitum carmichaelii* Debeaux by endophytic *Bacillus velezensis* YN-2-6S. *Biological Control* **201**:105690 DOI 10.1016/j.biocontrol.2024.105690.

Wang S, Tian J, Liu M. 2023. Research progress on pathogenic mechanism, toxin synthesis, prevention and control of C. longibracteata in sweet potato. *Jiangsu Journal of Agricultural Sciences* **39(05)**:1256–1264 DOI 10.3969/j.issn.1000-4440.2023.05.019.

Wang S, Tiian J, Liu M. 2023. Research progress on pathogenic mechanism, toxin synthesis, prevention and control of C. longibracteata in sweet potato. *Jiangsu Journal of Agricultural Sciences* **39(05)**:1256–1264 DOI 10.3969/j.issn.1000-4440.2023.05.019.

Wang Y, Wu LY, Wang HL, Jiang MY, Chen Y, Zheng XY, Li L, Yin Q, Han LZ, Bai L, Bian Y. 2025. Ligusticum chuanxiong: a chemical, pharmacological and clinical review. *Frontiers in Pharmacology* **16**:1523176 DOI 10.3389/fphar.2025.1523176.

Wei Z, Hu J, Ya Gu, Yin S, Xu Y, Jousset A, Shen Q, Friman V-P. 2017. Ralstonia solanacearum pathogen disrupts bacterial rhizosphere microbiome during an invasion. *Soil Biology and Biochemistry* **118**:8–17 DOI 10.1016/j.soilbio.2017.11.012.

Xian WD, Zhang XT, Li WJ. 2020. Research status and prospect of Chloroflexi. *Acta Microbiologica Sinica* **60(09)**:1801–1820 DOI 10.13343/j.cnki.wsxb.20200463.

Xing ZW, Chen Y, Chen JR, Peng C, Peng F, Li D. 2024. Metabolomics integrated with mass spectrometry imaging reveals novel action of tetramethylpyrazine in migraine. *Food Chemistry* **460**:140614 DOI 10.1016/j.foodchem.2024.140614.

Yin C, Casa Vargas JM, Schlatter DC, Hagerty CH, Hulbert SH, Paulitz TC. 2021. Rhizosphere community selection reveals bacteria associated with reduced root disease. *Microbiome* **9**(**1**):86 DOI 10.1186/s40168-020-00997-5.

Yu Y, Gui Y, Li Z, Jiang C, Guo J, Niu D. 2022. Induced systemic resistance for improving plant immunity by beneficial microbes. *Plants* **11**(**3**):386 DOI 10.3390/plants11030386.

Zanon MSA, Cavaglieri LR, Palazzini JM, Chulze SN, Chiotta ML. 2024. Bacillus velezensis RC218 and emerging biocontrol agents against Fusarium graminearum and Fusarium poae in barley: *in vitro*, greenhouse and field conditions. *International Journal of Food Microbiology* **114**:e110580 DOI 10.1016/j.ijfoodmicro.2024.110580.

Zhang F, Jin C, Hu R, Li Z, Hu S, Zhang Y, Zhang C. 2023. Rapid detection of *Fusarium fujikuroi* in rice seeds and soaking water samples based on recombinase polymerase amplification-lateral flow dipstick. *Plant Pathology* **73**(**3**):590–601 DOI 10.1111/ppa.13831.

Zhao J, Liu X, Hou L, Xu G, Guan F, Zhang W, Luo H, Wu N, Yao B, Zhang C, Delaplace P, Tian J. 2024. The seed endophytic microbe Microbacterium testaceum M15 enhances the cold tolerance and growth of rice (*Oryza sativa* L.). *Microbiological Research* **39**:127908 DOI 10.1016/j.micres.2024.127908.

Zhou YY, Jiang P, Ding YY, Zhang YP, Yang S, Liu XH, Cao CX, Luo GW, Ou LJ. 2025. Deciphering the distinct associations of rhizospheric and endospheric microbiomes with capsicum plant pathological status. *Microbial Ecology* **88**(**1**):1 DOI 10.1007/s00248-025-02499-z.

Zhou X, Zhang J, Khashiu Rahman M, Gao D, Wei Z, Wu F, Dini-Andreote F. 0000. Interspecific plant interaction *via* root exudates structures the disease suppressiveness of rhizosphere microbiomes. *Molecular Plant* **16**(**5**):849–864 DOI 10.1016/j.molp.2023.03.009.

Zhu T, Li L, Petridis A, Xydis G, Ren M. 2022. First report of fusarium asiaticum causing stem rot of ligusticum chuanxiong in China. *Plant Disease* **106**:325 DOI 10.1094/pdis-05-21-1026-pdn.